AGU PUBLICATIONS

JGR

Journal of Geophysical Research: Solid Earth

RESEARCH ARTICLE
10.1002/2013JB010579

Key Points:
- New streaming potential coefficient apparatus
- New transient methodology
- Initial data show extremely high quality data even to high salinities

Correspondence to:
P. W. J. Glover,
p.w.j.glover@leeds.ac.uk

Citation:
Walker, E., P. W. J. Glover, and J. Ruel (2014), A transient method for measuring the DC streaming potential coefficient of porous and fractured rocks, *J. Geophys. Res. Solid Earth*, *119*, 957–970, doi:10.1002/2013JB010579.

Received 2 AUG 2013
Accepted 16 JAN 2014
Accepted article online 20 JAN 2014
Published online 15 FEB 2014

A transient method for measuring the DC streaming potential coefficient of porous and fractured rocks

E. Walker[1], P. W. J. Glover[1,2], and J. Ruel[3]

[1]Département de géologie et de génie géologique, Université Laval, Québec, Quebec, Canada, [2]School of Earth and Environment, University of Leeds, Leeds, UK, [3]Département de génie méchanique, Université Laval, Québec, Quebec, Canada

Abstract High-quality streaming potential coupling coefficient measurements have been carried out using a newly designed cell with both a steady state methodology and a new pressure transient approach. The pressure transient approach has shown itself to be particularly good at providing high-quality streaming potential coefficient measurements as each transient increase or decrease allows thousands of measurements to be made at different pressures to which a good linear regression can be fitted. Nevertheless, the transient method can be up to 5 times as fast as the conventional measurement approaches because data from all flow rates are taken in the same transient measurement rather than separately. Test measurements have been made on samples of Berea and Boise sandstone as a function of salinity (approximately 18 salinities between 10^{-5} mol/dm^3 and 2 mol/dm^3). The data have also been inverted to obtain the zeta potential. The streaming potential coefficient becomes greater (more negative) for fluids with lower salinities, which is consistent with existing measurements. Our measurements are also consistent with the high-salinity streaming potential coefficient measurements made by Vinogradov et al. (2010). Both the streaming potential coefficient and the zeta potential have also been modeled using the theoretical approach of Glover (2012). This modeling allows the microstructural, electrochemical, and fluid properties of the saturated rock to be taken into account in order to provide a relationship that is unique to each particular rock sample. In all cases, we found that the experimental data were a good match to the theoretical model.

1. Introduction

Measurement of the electrokinetic and electrical properties of porous media is becoming increasingly more important in a wide range of research domains. Interest is particularly strong in the Earth sciences, where there are applications in hydrocarbon exploration and production [e.g., *Saunders et al*., 2008], water reservoir management [*Dupuis et al*., 2009; *Ishido and Pritchett*, 1999; *Titov et al*., 2005], the remediation of polluted soils [*Shapiro and Probstein*, 1993; *Maineult et al*., 2006; *Minsley et al*., 2007], and the prediction of volcanic [*Ishido*, 2004; *Revil et al*., 2002, 2003; *Aizawa et al*., 2005] and seismic [e.g., *Mizutani et al*., 1976] activity. There are also important commercial applications in polymer sciences [*Kocer and Weiland*, 2013], membrane sciences [*Szymczyk et al*., 2013], catalysis [*Zhang and Catchmark*, 2011], microfluidics [*Cho et al*., 2012], and food science [*Jindal et al*., 2013].

The electrical conductivity of Earth materials varies by over 24 orders of magnitude and can be measured with high accuracy, making the measurement extremely sensitive. Furthermore, the electrical properties of rocks can be measured remotely using electromagnetic induction [e.g., *Ingham et al*., 2009]. By contrast, it is not possible to monitor the flow of fluids in the subsurface without using boreholes, and each one samples only one position in the heterogeneous and anisotropic rock mass where complex flow and other processes are occurring.

The importance of electrokinetic phenomena is that they link the electrical and fluid flow properties of the porous and fractured rocks [*Jouniaux and Ishido*, 2012]. They offer, in principle, the ability to use remotely measured high-quality electrical measurements to monitor the presence and movement of fluids in the subsurface indirectly. Those mobile fluids may be associated with a water or hydrocarbon reservoir [*Saunders et al*., 2008], a pollutant plume [*Shapiro and Probstein*, 1993], new hydrothermal circulation stemming from the emplacement of new magma in a volcano [*Revil et al*., 2002], or fluid ingress into a fault that is in a critical earthquake state [*Mizutani et al*., 1976].

©2014. American Geophysical Union. All Rights Reserved.

Although this paper concerns itself with using slowly varying transient pressure variations to measure a steady state streaming potential, there have previously been several studies of transient streaming potentials and streaming potentials that result from harmonic flows in order to study the nature of the transient streaming potential or to measure the frequency-dependent streaming potential. A full review of these studies can be found in *Glover et al.* [2012b, 2012c].

In this paper we present an apparatus for measuring the DC streaming potentials on cylindrical rock cores (or samples of any other porous medium) that are saturated with aqueous fluids. The apparatus, which is also capable of measuring the complex electrical properties (conductivity, resistivity, or permittivity) of the sample as a function of applied electrical frequency between 1 mHz and 20 MHz, differs little from a number of such existing apparatuses, combining and extending the best aspects of previous designs. We have also developed a new methodology for making streaming potential coefficient measurements that employs a transiently varying fluid pressure difference instead of the steady state flow [*Jouniaux et al.*, 2000] or continuous ultralow frequency harmonic flows [*Revil et al.*, 2002] that have been used previously. Other recent studies of importance include those of *Allègre et al.* [2010, 2012] and *Jouniaux et al.* [2009], the latter of which uses measurements in both directions. This new approach has the advantage of providing high-quality measurements extremely quickly and allowing higher quality measurements to be made at high fluid salinities where streaming potentials are extremely low.

2. Apparatus and Experimental Methodology

Figure 1 shows the new apparatus. Most of the cell is made from engineering polymers. The central bore is large such that the pressure drop between the position of the lower electrode and the lower pressure transducer is negligible. The electrodes are inserted at an angle in order that gas bubbles can be removed easily from the flow path. The electrodes themselves are leak-free nonpolarizing reference Ag/AgCl electrodes (Warner Instruments 69-0053) with polyetheretherketone (PEEK®) bodies, a diameter of 1 mm, and an overall length of 100 mm. The electrodes are placed such that their porous tips are close to but not within the main flow path. Inserting the electrodes into the main flow path caused lower and erratic measured streaming potentials. The measured potentials were amplified by custom-designed amplifiers before being logged by a National Instruments DAQBoard NI USB6229 USB logger and PC running LabView Signal Express. The signals from each of two high-quality pressure transducers (Omega PX302 calibrated to an Endress and Hauser Deltabar S PMD75 secondary calibration standard) were also amplified by individual custom-designed amplifiers before being logged. A differential pressure transducer was added to the experimental setup for some measurements. The amplifiers are not strictly needed for the majority of the measurements made with the rig. However, the use of amplifiers enables us to extend the range of possible measurements (i) for high-salinity fluids, where the streaming potential is extremely low [*Vinogradov et al.*, 2010], or (ii) for low-salinity fluids, where the pressure difference required to generate a streaming potential is very low.

The electrical conductivity and pH of the fluids leaving the cell were also measured, together with their temperature and the temperature of the apparatus itself. Figure 1 incorporates flow loops associated with each measurement methodology, using the pump for steady state measurements and the high-pressure reservoir for the transient measurements. The entire apparatus was enclosed in a Faraday cage to remove unwanted noise.

In steady state measurements, streaming potential and fluid pressure difference measurements are usually made at between four and eight steady flow rates that are imposed using a pump. Some laboratories make measurements while fluid flows through the rock at several flow rates in each direction [*Revil et al.*, 2002; *Jouniaux et al.*, 2009], while others make more measurements but with fluid flowing in only one direction [*Lorne et al.*, 1999a; *Jouniaux et al.*, 2000]. When the data are plotted on a graph of streaming potential against imposed fluid pressure difference, the gradient provides an accurate streaming potential coefficient. This approach is common within the literature [e.g., *Vinogradov et al.*, 2010; *Jouniaux et al.*, 2000; *Lorne et al.*, 1999a, 1999b]. The steady state method is extremely accurate for moderate salinities, taking about 5–10 min to obtain steady potential and pressure readings for each flow rate. The data are logged for a statistically reasonable period so that an average value with an improved precision and signal-to-noise ratio can be calculated. Since each streaming coupling coefficient determination can use up to 10 flow rates in each direction, a typical set of measurements might take about between 2 and 4 h after fluid equilibrium has been achieved.

©2014. American Geophysical Union. All Rights Reserved.

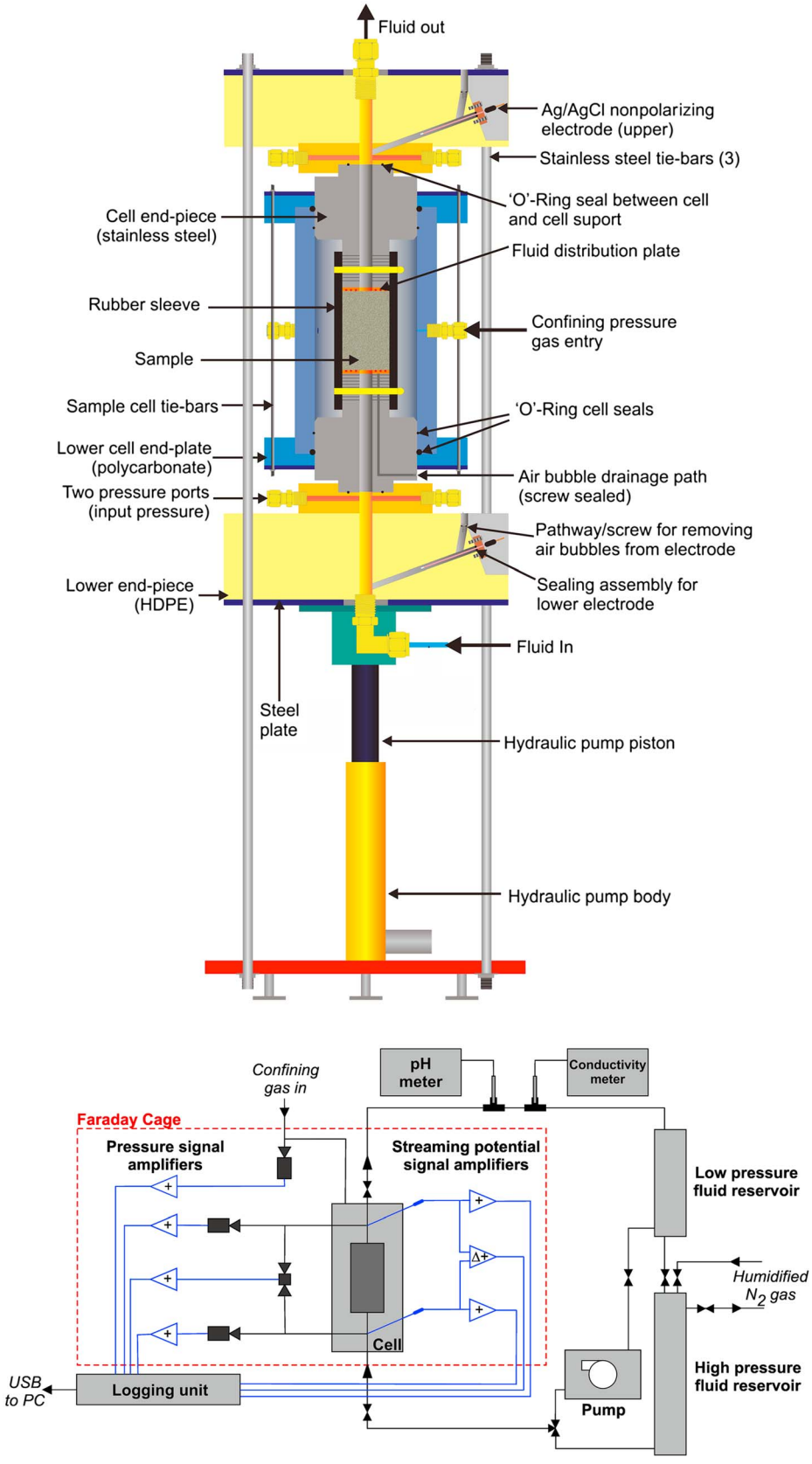

Figure 1. The new streaming potential coefficient cell (upper) and the simplified experimental arrangement (lower).

©2014. American Geophysical Union. All Rights Reserved.

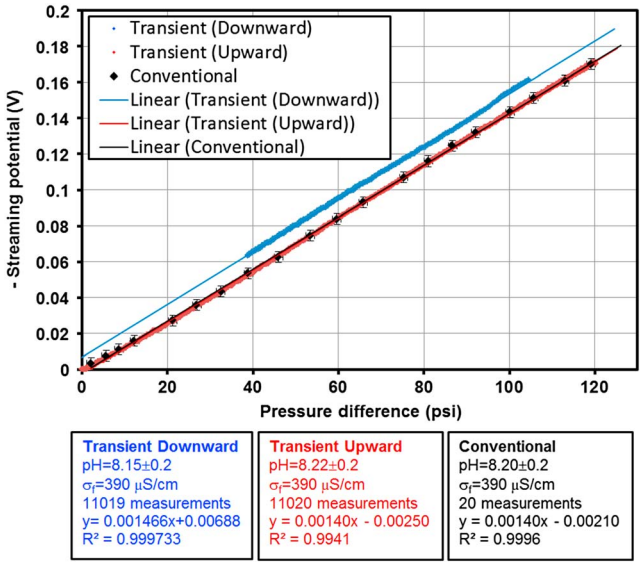

Figure 2. Measured streaming potential as a function of measured fluid pressure difference for the conventional approach (20 measurements, black symbols, *x* error ±1 psi, *y* error ± 3 mV), upward transient method (11,020 measurements, red symbols, no line), downward transient (11,019 measurements, blue symbols, no line). In each case linear regressions have been fitted to the data (red, black, and blue lines; see text). The sample is Berea sandstone (BR1) and the fluid was a 3×10^{-3} mol/dm^3 solution of NaCl after equilibration with the rock sample ($\sigma_f = 0.039$ S/m, pH 8.22). The permeability under these experimental conditions was 6.89×10^{-15} m^2 (6.98 mD).

Figure 2 shows an example of this approach using the new apparatus and a Pharmacia P500 pump on a sample of Berea sandstone (BR1) with a 3×10^{-3} mol/dm^3 solution of NaCl after equilibration with the rock sample ($\sigma_f = 0.039$ S/m, pH 8.22). Measurements were made for 20 flow rates in one direction. The measurements were made while flowing from the bottom of the sample to the top to avoid instabilities caused by the large internal bore of the cell. It is not common to make measurements at so many flow rates, but we wanted to maximize the precision of the measurement as we knew we wanted to compare it to measurements under the same conditions but made with the pressure transient approach. The measurements took just over 3 h. The resulting linear fit is extremely good ($R^2 = 0.9996$), and the calculated streaming potential coefficient is 1.40 mV/psi (2.03×10^{-7} V/Pa).

The problem with the steady state approach becomes apparent at very high salinities. At very low salinities the streaming potential coefficient is of the order of 10^{-5} V/Pa, requiring only a small pressure difference to give a streaming potential of sufficient size to measure with accuracy (1 kPa gives 10 mV). However, at high salinities the streaming potential coefficient is of the order of 10^{-10} V/Pa, requiring pressures of the order of 100 MPa to give a streaming potential of about 10 mV. Pumps that can generate fluid pressures of this order of magnitude are not commonly available.

In the pressure transient methodology a high-pressure reservoir is filled with pore fluid that has already been equilibrated with the rock sample. The reservoir is pressurized using humidified nitrogen to a predetermined pressure between 5 and 15 MPa (or higher if highly saline fluids are being flowed). The test is started by starting the logger and equalizing the pressure across the sample. A valve between the high-pressure reservoir and the sample is opened, resulting in a gradual increase in pressure across the sample until pressure equilibrium has been attained. A fluid permeability measurement is taken at this point. For us, the transient increase took approximately 100 s, during which more than 10,000 measurements of pressure and streaming potential were taken. The input valve was then closed, and logging continued during the transient exponential decrease of pressure across the sample. Once again, this process took about 100 s, and a similar number of measurements were taken. Once the pressure decrease had progressed to within a few percent of its asymptotic steady state value, the pressure across the sample was equalized and the logger stopped.

The zero flow and steady state flow pressures and potentials were used to zero the data, and a plot of the streaming potential against the fluid pressure difference for both the transient increase and the decrease was generated so that an accurate streaming potential coefficient could be determined by linear regression on each of the increasing and decreasing data sets. Figure 2 shows upward and downward transient data for the same rock/fluid combination that has previously been measured using the conventional methodology. In fact, the transient data were taken just after the conventional data. Linear regression lines have been fitted to both sets of data. It can be seen that the downward transient data have a zero offset. Nonzero offsets occur when the data have not been properly zeroed, and in this case the data have deliberately not been zeroed in order that they can be distinguished easily from the other data in the figure.

©2014. American Geophysical Union. All Rights Reserved.

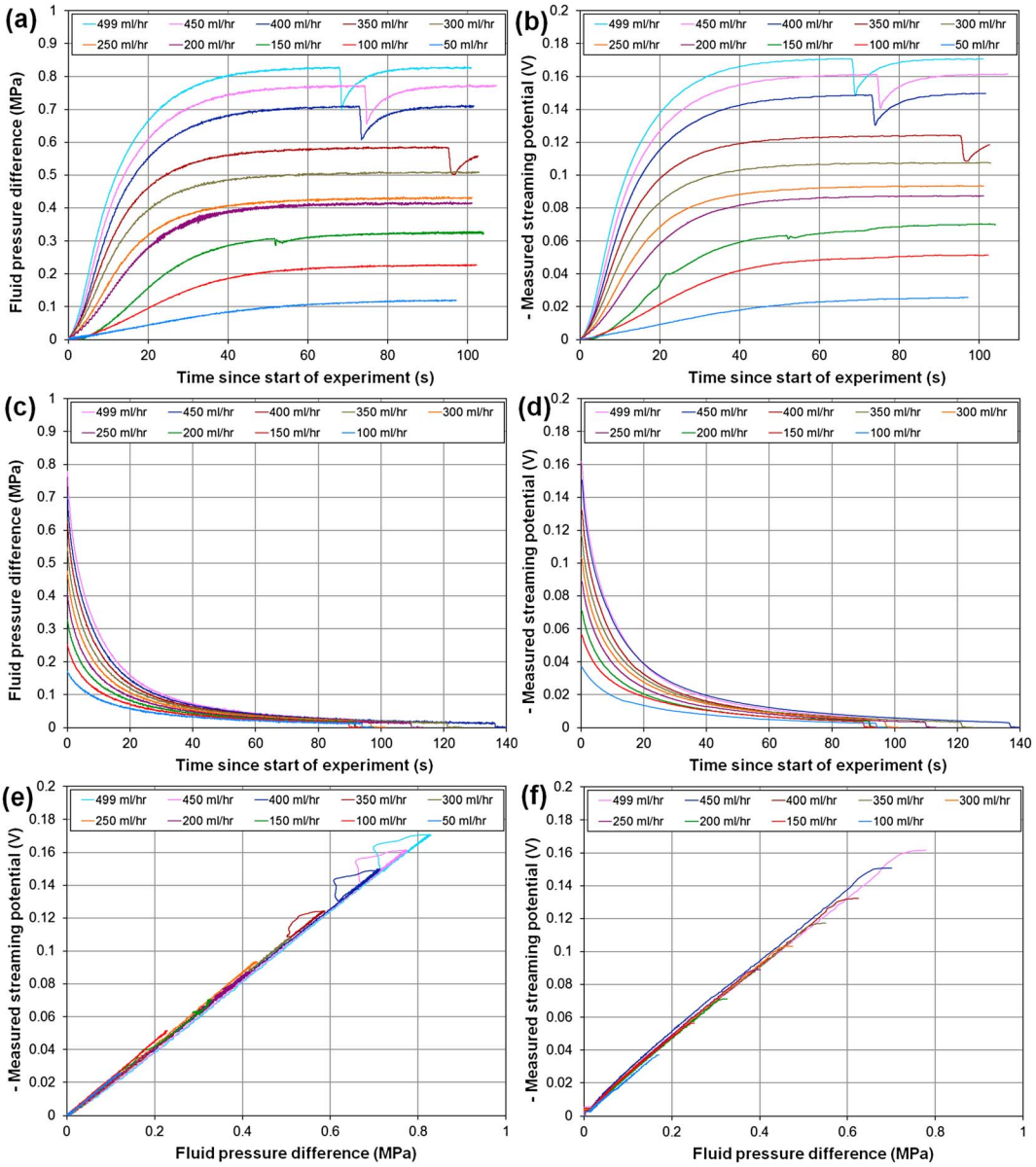

Figure 3. Upward and downward transient data made with a number of different flow rates. (a and b) Measured fluid pressure difference and streaming potential, respectively, as a function of duration during the upward leg of the experiment (about 12,000 data points per curve); (e) cross plot of the same data. (c and d) Measured fluid pressure difference and streaming potential, respectively, as a function of duration during the downward leg of the experiment (about 14,000 data points per curve); (f) cross plot of those data.

The upward transient data conform to a linear fit which is extremely good ($R^2 = 0.9941$), and the calculated streaming potential coefficient is exactly the same as that for the conventional measurement 1.40 mV/psi (2.03×10^{-7} V/Pa). The downward transient data also conform to a good linear fit ($R^2 = 0.9997$), and the calculated streaming potential coefficient 1.466 mV/psi (2.13×10^{-7} V/Pa) is almost the same as for the upward transient measurement and the conventional measurement. It is clear, therefore, that the data taken during the pressure increase and the pressure decrease agree very well with each other and with measurements on the same sample taken using the conventional approach. The difference here is that the conventional approach calculates the streaming potential coefficient using measurements of streaming potential at 20 different flow rates and took over 3 h to measure, whereas the transient approach calculates the streaming potential coefficient using over 20,000 measurements of streaming potential and differential fluid pressure and was completed within 5 min.

©2014. American Geophysical Union. All Rights Reserved.

Table 1. Sample Details for the Experimental Measurements and Parameters Used in the Theoretical Model[a]

Parameter	Symbol	Berea Sandstone BR1	Boise Sandstone B1II	Units	Comments
Rock sample properties					
Modal grain size (diameter)	d	265	739	μm	from laser diffractometry measurements
Cementation exponent	m	1.80	1.85	(−)	calculated from impedance measurements of the sample
Formation factor	F	10.46	6.31	(−)	calculated from impedance measurements of the sample
Porosity	ϕ	0.266	0.3002	(−)	from mercury porosimetry, used in modeling
		0.272	0.3695		from helium pycnometry
Permeability to pore fluid	k	6.89×10^{-15}	1.35×10^{-12}	m^2	measured during the streaming potential measurement, the lower value was measured with low-salinity pore fluids and the higher with high-salinity pore fluids
			2.08×10^{-12}		
Surface conductivity	Σ_s	2.6×10^{-3}	3.26×10^{-3}	S/m	calculated from impedance measurements of the sample
Modeling parameters					
Surface site density	Γ_o	NA	*10*[b]	$sites/nm^2$	within range of values for quartz made by independent measurements ($2.6–25$ $sites/nm^2$, see *Glover and Déry* [2010])
Binding constant for cation (sodium) adsorption on quartz	pK_{Me}	NA	*7.5*[b]	(−)	within range of values for quartz made by independent measurements (5.5–7.5; see *Glover and Déry* [2010])
Disassociation constant for dehydrogenization of silanol	$pK_{(-)}$	NA	*9*[b]	(−)	within range of values for quartz made by independent measurements (6.5–9; see *Glover and Déry* [2010])
Shear-plane distance	χ_ζ	NA	2×10^{-9}[b]	m	within range of values for silica made by independent measurements (2.4×10^{-10} to 2×10^{-9} m; see *Glover and Déry* [2010])
Surface conduction (proton)	Σ_s^{prot}	NA	2.4×10^{-8}	S	calculated from the surface site density and experimental determinations
Ionic Stern-plane mobility	β_s	NA	5×10^{-9}[b]	$m^2/s/V$	within range of values for quartz made by independent determinations (4×10^{-9} to 5.14×10^{-9} m; see *Glover and Déry* [2010])
Zeta potential offset	ζ_o	NA	−0.015	V	Chosen to allow a reasonable model fit at high salinities [see *Glover et al.*, 2012a]

[a]NA = not applicable—no modeling was carried out on this sample in this paper.
[b]Parameters which may be varied within the strict bounds set out in the comments column but were taken as constant in this work.

Figure 3 shows the measured streaming potentials and applied differential pressures during upward and downward transient experiments to different end pressures that were made during the validation of the transient method in order to confirm that the experimental system behaved reasonably and that nonlaminar flow was not affecting the results. These data were collected using a Pharmacia P500 dual piston pump to set up the pressure difference during the upward measurements rather than a gas-pressurized vessel that was used for later experiments. The data are "typical" rather than "high quality" and show a number of experimental artifacts, which are instructive for those also wishing to use this technique. For example, the upward measurements at a pump flow rate of 150 mL/h were affected by an erratic increase in pressure difference, and this is shown in both the streaming potential and pressure difference curves (Figures 3a and 3b) in a manner that is proportionate and does not result in a gross change of the streaming potential coefficient (Figure 3e). The erratic pressure difference was caused by the development of an air bubble inside one of the pump pistons. The upward measurement at a flow rate of 200 mL/h is slightly effected by 10 Hz noise which, in our case, arises from a radio/TV mast within 1 km of the laboratory in Québec. This source of noise was episodic and often overwhelmed our signal. We normally chose not to make measurements while it was active. It should be noted that an electrically quiet environment is essential for high-quality electrokinetic measurements. The flow rates above 340 mL/h all show a sudden loss of pressure that then recovers. These pressure loss events are caused by the changeover of piston barrels in the pump and cannot be avoided if a pump is used. It only affects the high flow rates because it is only these high flow rates that require a changeover of pistons within the duration of the experiment. Figure 3 shows that this artifact is present in both the measured pressure difference and the measured streaming potential. However, the effect is not proportional as can be seen in the derived streaming potential coefficient data (Figure 3e), where the effect is noted as an excursion to the left of the main trend that corrects itself.

The first and last of these artifacts is removed by our later use of a gas-pressurized cylinder as a source of driving pressure rather than the pump, while the broadcast noise problem was avoided by not making

©2014. American Geophysical Union. All Rights Reserved.

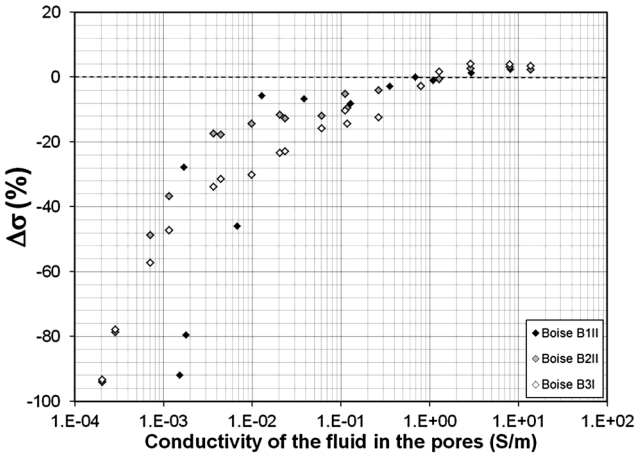

Figure 4. The percentage change in fluid conductivity between the fully equilibrated fluid and the original stock fluid for about 18 different salinities and three samples of Boise sandstone, according to $\Delta\sigma(\%) = 100 \times (\sigma_{stock} - \sigma_{actual})/\sigma_{actual}$.

measurements during its operation. All of the downward transient measurements in this data set behave very well and produce self-consistent straight lines when the streaming potential is plotted against the differential fluid pressure (Figures 3c, 3d, and 3f). The consistency between the gradients of all the curves in Figures 3e and 3f shows how well the streaming potential coupling coefficient can be measured using this technique.

3. Sample Material and Fluid Equilibration

Samples of Berea and Boise sandstone were used for the initial tests. A range of basic petrophysical tests were carried out on the samples (Table 1). The first of these rock types was chosen because it is a common reservoir analogue, with much other data available about it in the literature. Boise sandstone is less well studied. It is a highly permeable rock that we had available for frequency-dependent electrokinetic studies and was chosen to represent high-porosity, high-permeability rocks. Both steady state and transient measurements were carried out on a number of samples. Streaming potential measurements were carried out for 18 salinities between about 10^{-5} mol/dm^3 and 2 mol/dm^3, at a nominal pH of 7. In each case the solutions had to be equilibrated with the rock sample in order to obtain stable, repeatable streaming potential coefficient values. The equilibration was carried out by changing the fluid and then recycling the new fluid through the sample until at least 50 pore volumes had been flowed and after all the pore fluid reservoir had passed through the sample at least twice. The electrical conductivity and pH of the fluids exiting the sample were measured as shown in Figure 1.

During equilibration, the electrical conductivity and pH of the evolved fluid was found to change. Consequently, these two parameters were used to judge the equilibration of the pore fluid with the sample. It was found that low-salinity fluids increased in salinity by as much as 1 order of magnitude for low-salinity fluids, while the pH could change by up to 1.5 points. Figure 4 shows the percentage change in fluid conductivity between the fully equilibrated fluid and the original stock fluid for about 18 different salinities and three rock samples, according to $\Delta\sigma(\%) = 100 \times (\sigma_{stock} - \sigma_{actual})/\sigma_{actual}$. The figure shows clearly that low-salinity bulk fluids increase in salinity, and hence conductivity, when equilibrated with the rock sample, whereas at high salinities there is some slight evidence that the opposite effect is taking place. The size of the effect at low salinities is such that it is impossible to have an ultralow-salinity fluid in the pore space in order to make a measurement because equilibration with the matrix increases its salinity and conductivity. This effect is sufficiently important that we not only need to equilibrate our pore fluids fully with the rock under study but we need to analyze the resulting streaming potential coefficient measurements with respect to the salinities, conductivities, and pHs of the actual fluid in the rock during the measurement rather than those of the bulk fluid. This implies that the electrical conductivity and pH of the evolved fluids should be measured at the outlet of the sample in real time.

All the results presented in this work are plotted against the salinity of the fluid evolving from the sample at the time of the streaming potential measurement after full equilibration had been achieved, and if one wanted to plot the data as a function of electrical resistivity or pH, one should also use the electrical resistivity or pH of the fluid evolving from the sample at the time of the streaming potential measurement.

The achievement of equilibration has been judged by stability in the pH and electrical conductivity of the evolving fluids. However, the question arises how long that takes. Unfortunately, we did not study the equilibration time explicitly. However, initially we flowed at least 50 pore volumes through the rock, which for the Berea sample took over 16 h. We noticed that equilibration was slowest for low-salinity fluids and fastest

©2014. American Geophysical Union. All Rights Reserved.

for high-permeability rocks through which we could flow fluids more quickly. Sometimes we could attain equilibration for the Berea sandstones within 5 h when the fluid salinities were fairly high and only incrementally changed from the previous fluid and as fast as 30 min in the case of the high-permeability Boise sandstone. Equilibration is, then, more controlled by the volume of fluid that has passed through the sample than the time it takes to do so.

4. Data Analysis Methodology

There are two data analysis pathways—experimental and theoretical.

In the experimental part (section 5—Initial Results) measurements are made to find (i) the streaming potential coefficient, (ii) fluid pH, (iii) fluid conductivity, (iv) the apparent (or instantaneous) formation factor as a function of salinity, and (v) the formation factor at high salinity. These are independent measurements that are used together with values of fluid permittivity and viscosity from empirical relationships in order to calculate a zeta potential using the standard Helmholtz-Smoluchowski equation but with the fluid conductivity element modified using Overbeek's correction to account for the extra conduction provided by the diffuse layer at low salinities [*Pozzi and Jouniaux*, 1994; *Jouniaux and Pozzi*, 1995; *Alkafeef and Alajmi*, 2006; *Wang and Hu*, 2012]. The relevant equation is

$$\zeta = \frac{C_s \eta_f \sigma_f}{\varepsilon_f} \frac{F}{F_{\text{inst}}}, \tag{1}$$

where the formation factor is defined as the ratio of the electrical conductivity of the fluid to that of the fluid saturated rock, F is the formation factor of the sample at high salinity (where the surface conduction is insignificant compared to conduction through the bulk fluid), F_{inst} is the formation factor of the sample at each salinity (where there may be a significant contribution of surface conduction to the total fluid conductivity), η_f is the viscosity of the equilibrated pore fluid, ε_f is the permittivity of the equilibrated pore fluid, σ_f is the electrical conductivity of the equilibrated pore fluid, ζ is the zeta potential, and C_s is the measured streaming potential coefficient. The ratio of the two formation factors is termed the Overbeek correction.

This is a "top-down" approach to finding the zeta potential in that the zeta potential is derived solely from experimental measurements.

In the theoretical approach (section 6—Theoretical Modeling) the approach is completely different and does not rely on knowing the streaming potential coefficient in advance. It calculates both the zeta potential and surface conduction using the electrochemical approach originally pioneered by *Glover et al*. [1994], *Pride* [1994], *Revil and Glover* [1997, 1998], and *Revil et al*. [1999]. The input parameters are (i) the surface site density, (ii) the binding constant for cation (sodium) adsorption on quartz, (iii) the disassociation constant for the dehydrogenization of silanol, (iv) the shear-plane distance, (v) the protonic surface conduction, and (vi) the ionic Stern-plane mobility. This is a "bottom-up" approach to finding the zeta potential in that the zeta potential is arrived at from the electrochemistry of the mineral-fluid interface.

Once the zeta potential is independently theoretically modeled, the streaming potential coefficient may be obtained from it by using the same equation that was used to calculate the experimental zeta potential but backward, i.e.,

$$C_s = \frac{\varepsilon_f \zeta}{\eta_f \sigma_f} \frac{F_{\text{inst}}}{F}. \tag{2}$$

However, we have preferred to use a modified form of the Helmholtz-Smoluchowski equation that was introduced by *Glover and Déry* [2010] in order to account for the functional dependence of the streaming potential coefficient on the grain size of the rock.

$$C_s = \frac{\mathrm{d}\varepsilon_f \zeta}{\eta_f (\mathrm{d}\sigma_f + 4\Sigma_s m F)}, \tag{3}$$

where d is the modal grain size, m is the cementation exponent, and Σ_s is the surface conductance (specific surface conductivity).

©2014. American Geophysical Union. All Rights Reserved.

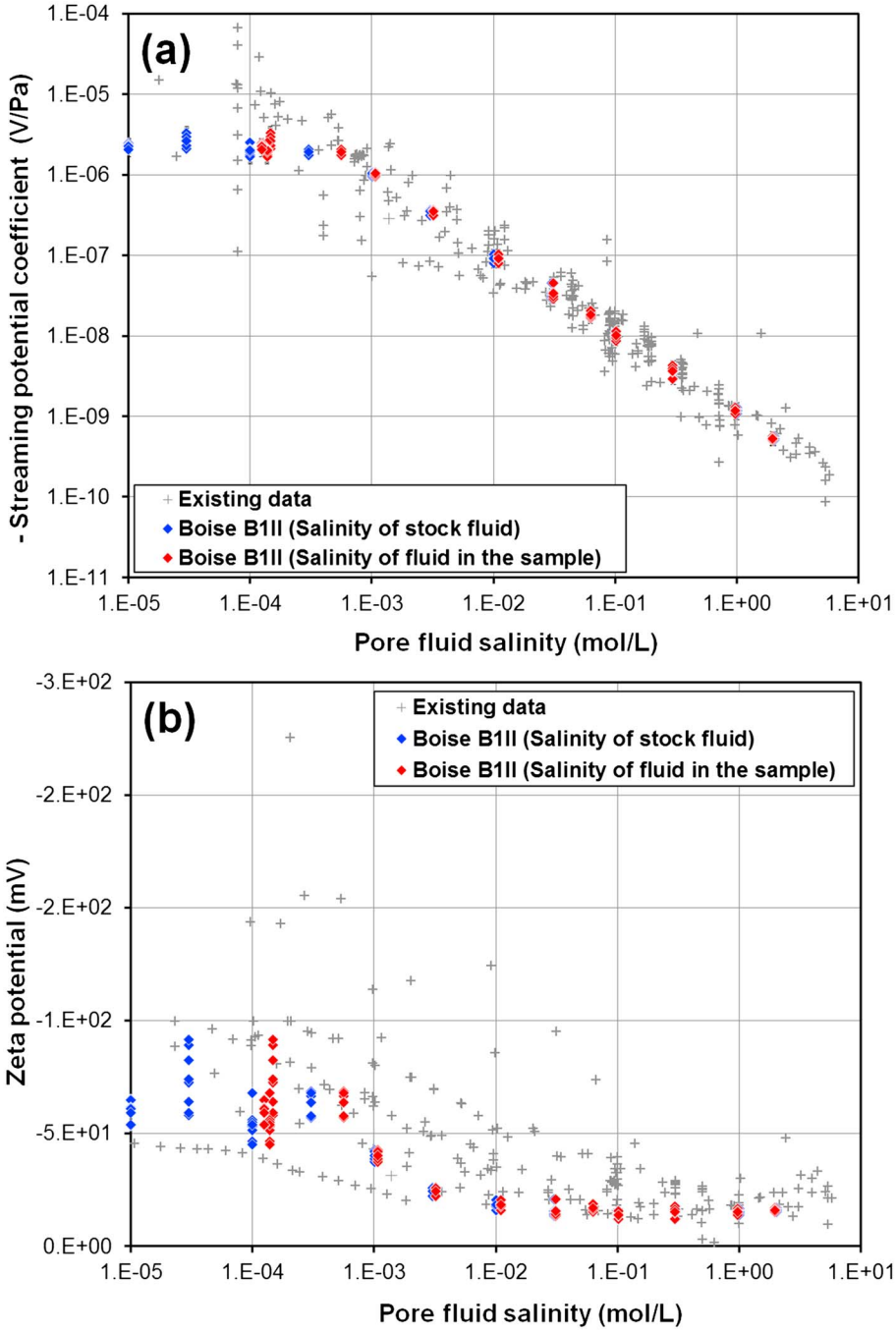

Figure 5. The (a) streaming potential coefficient and (b) zeta potential for a sample of Boise sandstone (B1II) while saturated with various salinities and pHs of aqueous NaCl (between 10^{-5} mol/dm^3 and 2 mol/dm^3 and pH approximately 6.88). The data are given with respect to salinity of the stock solution before equilibration of the fluid with the sample (open diamonds) and with respect to the fully equilibrated pore solution, with electrical conductivity, salinity, and pH measured as it leaves the sample during streaming potential measurements (solid diamonds). The zeta potential is calculated with equation (1) as described in the text. The crosses represent a database of undifferentiated measurements made on silica-based rock types measured previously (full details in *Glover et al.* [2012a]).

Equations (2) and (3) are, in fact, formally the same and differ only in that the former accounts for the extra conduction from surface conduction at low salinities in terms of the ratio of instantaneous to high-salinity formation factors, while the latter relates the surface conduction to grain size, surface conductance, cementation exponent, and formation factor. The advantage in using the *Glover and Déry* [2010] approach in the theoretical modeling is that the surface conduction is available from previous electrochemical modeling, while the

©2014. American Geophysical Union. All Rights Reserved.

modal grain size was available from laser diffractometry measurements on crushed samples and the cementation exponent and formation factor were already available at the experimental conditions.

Hence, there is no circular argument in the theoretical modeling, and the results of theoretical modeling and experimentally derived values for both the zeta potential and the streaming potential coefficient may be considered independent and can be compared.

5. Initial Results

Figure 5 shows the streaming potential coefficient and zeta potential of a sample of Boise sandstone (B1II) made with the new transient methodology. This is one typical data set from a number that have been measured on Berea, Boise, and Lochaline sandstones as a function of pore fluid type, salinity, and pH, and which will form the subject of future publications. The measurements shown here were made over a period of a couple of months; the duration is not controlled by the actual measurements, which are fairly fast, as previously described, but by the length of time it took to equilibrate each of the fluids with the rock sample. Figure 5 shows the difference between plotting the streaming potential coefficient data against the equilibrium fluid that is in the rock at the time of the streaming potential measurement (solid diamonds) and that of the bulk fluid (open diamonds) at the same temperature (25°C).

The parameters used in equation (1) to derive the zeta potential from the experimental streaming potential coefficient are (i) electrical permittivity, which was calculated for an aqueous NaCl solution for each salinity at 25°C using the unpublished method of Gary Olhoeft [e.g., *Glover et al*., 2012a], (ii) pore fluid viscosity, which was calculated for a NaCl solution for each salinity at 25°C using the method of *Phillips et al*. [1978], (iii) the fluid electrical conductivity, which was measured on the fluid leaving the sample at the time of the streaming potential measurement, (iv) the measured streaming potential coefficient, and (v) the experimentally determined instantaneous and high-salinity formation factors. Hence, the zeta potential is calculated using a number of independent measurements with two empirical relationships for fluid properties.

Figure 5 also shows the streaming potential and zeta potential data for a database of previous measurements on predominantly silica-based rocks (290 streaming potential coefficient and 269 zeta potential) compiled in *Glover et al*. [2012a]. We make no distinction in this figure between these measurements in order not to overcomplicate it, but full information can be found in *Glover et al*. [2012a]. It should be noted that there is considerable ambiguity whether some of the historic zeta potential data were derived from the standard Helmholtz-Smoluchowski equation with or without the Overbeek correction. What is more, some historic data make no distinction between stock and equilibrated pore fluids. This variability of approach may explain some of the scatter in the historic data and will lead to the zeta potential being underestimated progressively as salinities become weaker than 0.001 mol/L. However, most of the scatter is due to differences in fluid pH, a fluid property which is very important in electrokinetic research but which is often not measured or reported in papers. Figure 5 shows clearly that the new streaming potential coefficient and zeta potential measurements are consistent with those that have been derived previously and seem to have less scatter.

6. Theoretical Modeling

Between 1994 and 1998 a number of papers were published that allowed the modeling of the electrical double layer in rocks and which made it possible to calculate the steady state electrical conductivity of a rock including the contribution made by surface conduction [*Glover et al*., 1994; *Pride*, 1994; *Revil and Glover*, 1997, 1998; *Revil et al*., 1999]. This theoretical approach is based upon the electrochemical interactions that give rise to the electrical double layer at the interface between the rock matrix and the pore fluid. These papers also allowed the calculation of the zeta potential [*Revil et al*., 1999]. Unfortunately, Helmholtz-Smoluchowski's law could not then be used to obtain the streaming potential coefficient because it is only valid for capillary tubes. In the case of a porous medium the streaming potential coefficient is sensitive to its particular microstructure, which is described by its formation factor, cementation exponent, and porosity, as well as some measure of grain or pore size. Recently, *Glover and Déry* [2010] reported a method for incorporating these individual rock parameters in Helmholtz-Smoluchowski's law (equation (3) above and its analogues), which has led to a full electrochemical theory for the calculation of the streaming potential coefficient for individual rock samples [*Glover et al*., 2012a].

©2014. American Geophysical Union. All Rights Reserved.

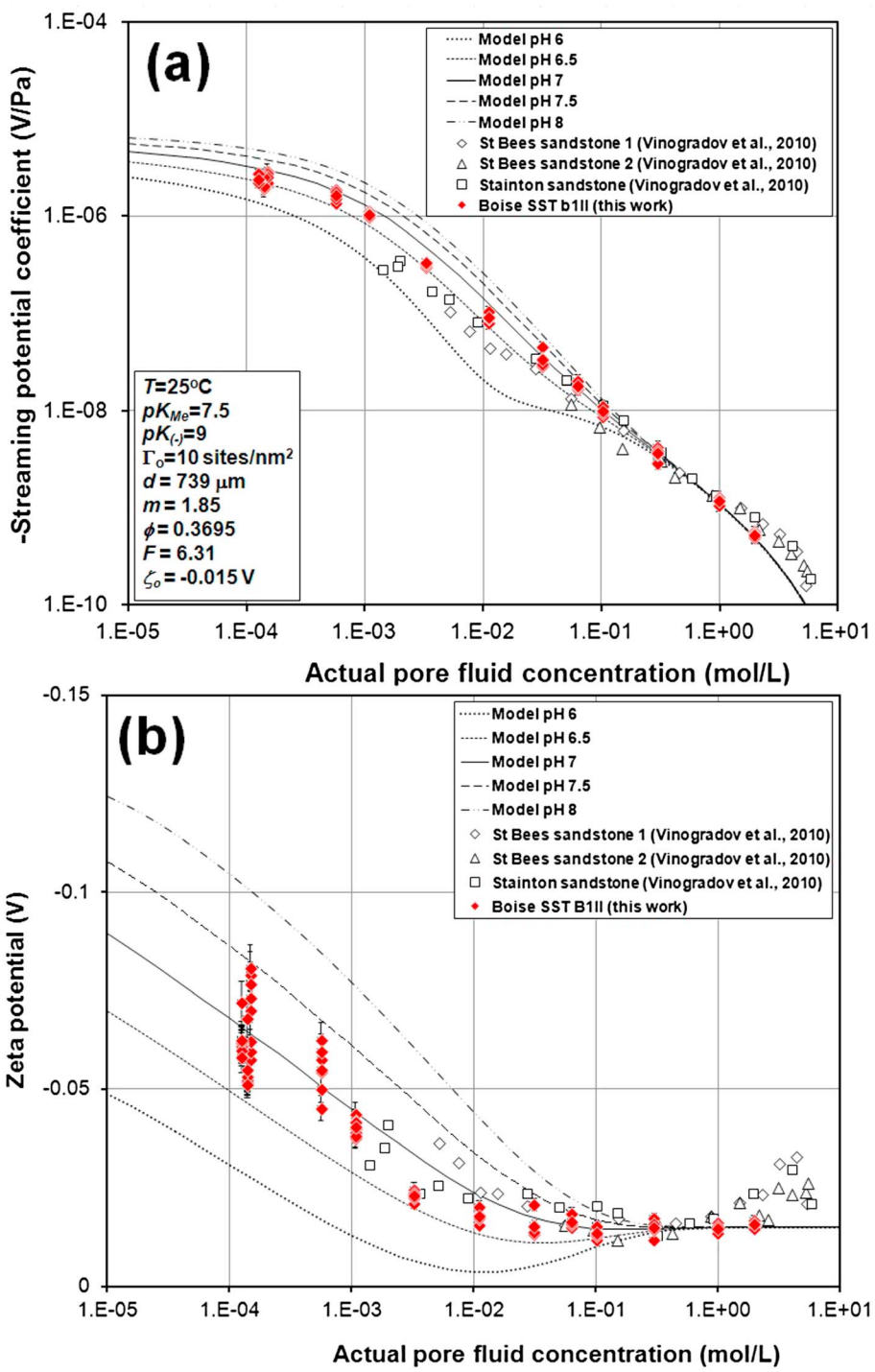

Figure 6. Comparison of the (a) measured streaming potential coefficient and (b) zeta potential for the sample of Boise sandstone (B1II) given in Figure 5 with the results of the *Glover et al.* [2012a] theoretical model. The model has been calculated for an aqueous solution of NaCl at 25°C with salinities between 10^{-5} mol/dm^3 and 2 mol/dm^3 and five pHs between 6 and 8 in increments of half a pH unit. The data are given with respect to salinity of the fully equilibrated pore solution in the sample at the time of the measurement of streaming potential. Modeling parameters are shown in the figure and also in Table 1.

We have used this model to calculate the zeta potential and streaming potential coefficient for individual rock samples measured in this work. A full description of the model can be found in *Glover et al.* [2012a] with additional information also in *Glover and Déry* [2010]. A comparison of the measured streaming potential and zeta potential data with curves generated from the theoretical model is given as Figure 6.

©2014. American Geophysical Union. All Rights Reserved.

The model curves have been calculated for aqueous NaCl fluid salinities between 10^{-5} mol/dm^3 and 10 mol/dm^3 and pH from 6 to 8. Table 1 contains the model parameters used to produce the models shown in Figure 6. No parameters in the model are freely adjustable. The microstructural parameters are fixed by the sample, while there are a number of parameters that are either fundamental constants, modeling variables (temperature and salinity), or constant electrochemical parameters such as the equilibrium constants that define the pH of the solution. There are five parameters that could be adjusted in a limited way if one wanted to fit the model to the data. However, we have not followed that approach. These electrochemical parameters describe the electrical double layer and are shown with superscripted letter b in Table 1. Each is adjustable within strict limits imposed by independent experimental measurements that are noted in Table 1 and discussed fully in *Glover et al*. [2012a]. In most cases, variation of these parameters within the given limits does not affect the model significantly. The approach we have used is to choose a typical constant value for each of the parameters marked with superscripted letter b within the range of experimentally determined values made by other researchers and discussed fully in *Glover et al*. [2012a] rather than let an automatic best fitting procedure find the values that best fit the model to the data. In this way, the model and the data remain independent.

In fact, the two parameters to which the model is most sensitive are the surface site density (Γ_o) and the disassociation constant for dehydrogenization of silanol ($pK_{(-)}$), while increasing the value of the shear-plane distance (χ_ζ) removes the pH dependence of the curves without significantly changing their position or gradient. Since there are strict limits on the adjustability of these modeling parameters, we are content that the quality of fit between the measured and theoretical curves in Figure 6 does not arise solely from freedom of fitting but is due to the known microstructural parameters for each rock sample.

The final parameter is the zeta potential offset ζ_o (Table 1). This parameter was invoked in the description of the theoretical model [*Glover and Déry*, 2010; *Glover et al*., 2012a] in order to ensure that the streaming potential can be modeled at high salinities ($C_f > 1$ mol/dm^3). It is added to the variable zeta potential calculated from the model using electrochemical considerations. In this work it is taken to be constant and equal to -15 mV.

Hence, it is clear that the new experimental data are also consistent with the results of the best theoretical model that is currently available. However, it is recognized that this model could be improved such that the zeta potential offset is not required in future.

7. Conclusions

A new apparatus and a new transient approach have been developed for the measurement of streaming potential coefficient in porous and fractured rocks. The apparatus and new methodology have been tested and found to produce high-quality data that (i) are statistically identical with those made using the conventional methodologies, (ii) are consistent with experimental data on other types of sandstone, and (iii) are also consistent with the theoretical model for streaming potential and zeta potential in porous rocks. A large number of measurements have been made using this technique on different types of sandstone for different fluid types, salinities, and pHs. These will be published in forthcoming papers.

During the analysis of the data it became clear that the salinity, electrical conductivity, and pH of the fluid in equilibrium with the rock sample when the streaming potential measurement is made can be significantly different from that of the initial stock solution. It is therefore recommended that all data from electrokinetic measurements in the laboratory are analyzed and presented with reference to the actual electrical conductivity, salinity, and pH of the fluid in the rock at the time of the measurement and leaving the sample, after full equilibration of the sample with the pore fluid, rather than the values measured on the bulk pore fluid before equilibration with the sample.

Comparison of the theoretical model with the experimentally derived data for both the streaming potential coefficient and the zeta potential shows clearly that the theoretical models that are based on electrochemical arguments are becoming very good at describing the experimental data. Problems remain, however, with the need to use a zeta potential offset in order for the high salinities to be modeled well. Further work is needed on the fluid viscosity and permittivity inputs to the model as the value of these parameters will be different in the Electrical Double Layer (EDL) [*Glover et al*., 2012a]. It is expected that the zeta potential offset will not be required when the correct viscosity and permittivities are used.

©2014. American Geophysical Union. All Rights Reserved.

At the least, we now have two ways of determining the zeta potential and streaming potential coefficients of rocks: by accurate experimental measurement using a developing protocol or by theoretical modeling. Both are quite complex. The experimental measurements should be done with accuracy and a care taken to use equilibrated fluids. The theoretical model has many input parameters, all of which need to be carefully chosen and justified.

One thing is certain; the effect of fluid equilibration, fluid conductivity, surface conductivity, and fluid pH are all important. It is strongly recommended that all of these parameters are carefully measured and controlled in any future experimental studies. We recognize, for example, that the lack of fluid pH control is the biggest factor leading to the large degree of scatter in historic zeta potential measurements.

Acknowledgments
The funding for this work was provided by the Natural Sciences and Engineering Research Council of Canada (NSERC) Discovery Grant Programme and a dowry from the University of Leeds.

References

Aizawa, K., et al. (2005), Hydrothermal system beneath Mt Fuji volcano inferred from magneto-tellurics and electric self-potential, *Earth Planet. Sci. Lett.*, *235*, 343–355, doi:10.1016/j.epsl.2005.03.023.

Alkafeef, S., and A. Alajmi (2006), Streaming potentials and conductivities of reservoir rock cores in aqueous and non-aqueous liquids, *Colloids Surf. A: Physicochem Eng. Aspects*, *289*, 141–148.

Allègre, V., L. Jouniaux, F. Lehmann, and P. Sailhac (2010), Streaming potential dependence on water-content in Fontainebleau sand, *Geophys. J. Int.*, *182*, 1248–1266.

Allègre, V., F. Lehmann, P. Ackerer, L. Jouniaux, and P. Sailhac (2012), Modelling the streaming potential dependence on water content during drainage: 1. A 1D modelling of SP using finite element method, *Geophys. J. Int.*, *189*, 285–295.

Cho, D., S. Lee, and M. W. Frey (2012), Characterizing zeta potential of functional nanofibers in a microfluidic device, *J. Colloid Interface Sci.*, *372*(1), 252–260.

Dupuis, J. C., K. Butler, A. Kepic, and B. Harris (2009) Anatomy of a seismo-electric conversion: Measurements and conceptual modeling in boreholes penetrating a sandy aquifer, *J. Geophys. Res.*, *114*, B10306, doi:10.1029/2008JB005939.

Glover, P. W. J., and N. Déry (2010), Dependence of streaming potential on grain diameter and pore radius for quartz glass beads, *Geophysics*, *75*(6), F225–241, doi:10.1190/1.3509465.

Glover, P. W. J., P. G. Meredith, P. R. Sammonds, and S. A. F. Murrell (1994), Ionic surface electrical conductivity in sandstone, *J. Geophys. Res.*, *99*(B11), 21,635–21,650.

Glover, P. W. J., E. Walker, and M. D. Jackson (2012a), Streaming-potential coefficient of reservoir rock: A theoretical model, *Geophysics*, *77*(2), D17–D43, doi:10.1190/GEO2011-0364.1.

Glover, P. W. J., J. Ruel, E. Tardif, and E. Walker (2012b), Frequency-dependent streaming potential of porous media—Part 1: Experimental approaches and apparatus design, *Int. J. Geophys.*, *2012*, Article 846204, doi:10.1155/2012/846204.

Glover, P. W. J., E. Walker, J. Ruel, and E. Tardif (2012c), Frequency-dependent streaming potential of porous media—Part 2: Experimental measurement of unconsolidated materials, *Int. J. Geophy.*, *2012*, Article 728495, doi:10.1155/2012/728495.

Ingham, M. R., H. M. Bibby, W. Heise, K. A. Jones, P. Cairns, S. Dravitzki, S. L. Bennie, T. G. Caldwell, and Y. A. Ogawa (2009), Magneto-telluric study of Mount Ruapehu volcano New Zealand, *Geophys. J. Int.*, *179*, 887–904, doi:10.1111/gji.2009.179.issue-2.

Ishido, T. (2004) Electrokinetic mechanism for the w-shaped self-potential profile on volcanoes, *Geophys. Res. Lett.*, *31*, L15616, doi:10.1029/2004GL020409.

Ishido, T., and J. W. Pritchett (1999), Numerical simulation of electro-kinetic potentials associated with subsurface fluid flow, *J. Geophys. Res. B*, *104*(B7), 15,247–15,259.

Jindal, M., V. Kumar, V. Rana, and A. K. Tiwary (2013), Physico-chemical, mechanical and electrical performance of bael fruit gum-chitosan IPN films, *Food Hydrocolloids*, *30*(1), 192–199.

Jouniaux, L., and T. Ishido (2012), Electro-kinetics in Earth sciences: A tutorial, *Int. J. Geophys.*, *2012*, 286107, doi:10.1155/2012/286107.

Jouniaux, L., and J. P. Pozzi (1995), Streaming potential and permeability of saturated sandstones under triaxial stress: Consequences for electrotelluric anomalies prior to earthquakes, *J. Geophys. Res.*, *100*(B6), 10,197–10,209, doi:10.1029/95JB00069.

Jouniaux, L., M. L. Bernard, M. Zamora, and J. P. Pozzi (2000), Streaming potential in volcanic rocks from Mount Pelée, *J. Geophys. Res.*, *105*(B4), 8391–8401.

Jouniaux, L., A. Maineult, V. Naudet, M. Pessel, and P. Sailhac (2009), Review of self-potential methods in hydrogeophysics, *C. R. Geosci.*, *341*, 928–936.

Kocer, B., and L. M. Weiland (2013), Experimental investigation of the streaming potential hypothesis for ionic polymer transducers in sensing, *Smart Mater. Struct.*, *22*(3), 035,020, doi:10.1088/0964-1726/22/3/035020.

Lorne, B., F. Perrier, and J.-P. Avouac (1999a), Streaming potential measurements: 1 Properties of the electrical double layer from crushed rock samples, *J. Geophys. Res.*, *104*(B8), 17,857–17,877, doi:10.1029/1999JB900156.

Lorne, B., F. Perrier, and J.-P. Avouac (1999b), Streaming potential measurements: 2 Relationship between electrical and hydraulic flow patterns from rock samples during deformation, *J. Geophys. Res.*, *104*(B8), 17,879–17,896, doi:10.1029/1999JB900155.

Maineult, A., Y. Bernabé, and P. Ackerer (2006), Detection of advected, recating redox fronts from self-potential measurements, *J. Contam. Hydrol.*, *86*, 32–52.

Minsley, B. J., J. Sogade, and F. D. Morgan (2007), Three-dimensional self-potential inversion for subsurface dnapl contaminant detection at the savannah river site, South Carolina, *Water Resour. Res.*, *43*, W04429, doi:10.1029/2005WR003996.

Mizutani, H., T. Ishido, T. Yokokura, and S. Ohnishi (1976), Electro-kinetic phenomena associated with earthquakes, *Geophys. Res. Lett.*, *3*(7), 365–368, doi:10.1029/GL003i007p00365.

Phillips, S. L., H. Ozbek, and R. J. Otto (1978), Basic energy properties of electrolytic solutions database, paper presented at Sixth International CODATA Conference, Santa Flavia, Sicily, Italy, 2–25 May. [Available at http://www.etde.org/etdeweb/purl.cover.jsp?purl=/6628103-xaRVpW/.]

Pozzi, J.-P., and L. Jouniaux (1994), Electrical effects of fluid circulation in sediments and seismic prediction, *C. R. Acad. Sci. Ser. II*, *318*(1), 73–77.

Pride, S. (1994), Governing equations for the coupled electromagnetics and acoustics of porous media, *Phys. Rev. B: Condens. Matter Mater. Phys.*, *50*, 15,678–15,696, doi:10.1103/PhysRevB.50.15678.

Revil, A., and P. W. J. Glover (1997), Theory of ionic surface electrical conduction in porous media, *Phys. Rev. B: Condens. Matter Mater. Phys.*, *55*, 1757–1773, doi:10.1103/PhysRevB.55.1757.

©2014. American Geophysical Union. All Rights Reserved.

Revil, A., and P. W. J. Glover (1998), Nature of surface electrical conductivity in natural sands, sandstones, and clays, *Geophys. Res. Lett.*, *25*(5), 691–694, doi:10.1029/98GL00296.

Revil, A., P. A. Pezard, and P. W. J. Glover (1999), Streaming potential in porous media. I Theory of the zeta-potential, *J. Geophys. Res.*, *104*(B9), 20,021–20,031, doi:10.1029/1999JB900089.

Revil, A., D. Hermitte, E. Spangenberg, and J. J. Cochemé (2002), Electrical properties of zeolitized volcaniclastic materials, *J. Geophys. Res.*, *107*(B8), 2168, doi:10.1029/2001JB000599.

Revil, A., G. Saracco, P. Labazuy (2003), The volcano-electric effect, *J. Geophys. Res.*, *108*(B5), 2251, doi:10.1029/2002JB001835.

Saunders, J. H., M. D. Jackson, and C. C. Pain (2008), Fluid flow monitoring in oil fields using downhole measurements of electro-kinetic potential, *Geophysics*, *73*(5), E165, doi:10.1190/1.2959139.

Shapiro, A. P., and R. F. Probstein (1993), Removal of contaminants from saturated clay by electro-osmosis, *Environ. Sci. Technol.*, *27*, 283–291, doi:10.1021/es00039a007.

Szymczyk, A., Y. I. Dirir, M. Picot, I. Nicolas, and F. Barrière (2013), Advanced electro-kinetic characterization of composite porous membranes, *J. Membr. Sci.*, *429*, 44–51.

Titov, K., A. Revil, P. Konasovsky, S. Straface, and S. Troisi (2005), Numerical modeling of self-potential signals associated with a pumping test experiment, *Geophys. J. Int.*, *162*, 641–650, doi:10.1111/gji.2005.162.issue-2.

Vinogradov, J., M. Z. Jaafar, and M. D. Jackson (2010), Measurement of streaming potential coupling coefficient in sandstones saturated with natural and artificial brines at high salinity, *J. Geophys. Res. B*, *115*, B12204, doi:10.1029/2010JB007593.

Wang, J., and H. Hu (2012), The determination of electro-kinetic coupling co-efficient and zeta potential of rock samples by electro-kinetic measurements, *Adv. Mater. Res.*, *516–517*, 1870–1873.

Zhang, J., and J. M. Catchmark (2011), A catalytically powered electro-kinetic lens: Toward channel-less microfluidics, *Microfluid. Nanofluid.*, *10*(5), 1147–1151.

©2014. American Geophysical Union. All Rights Reserved.